TechnoChem

International Journal of TechnoChem Research
ISSN:2395-4248 www.technochemsai.com
Vol.02, No.03, pp 181-188, 2016

Effect of Fe(II) and Fe(III) doping in Ammonium Dihydrogen Phosphate Crystals

M. Dhanalakshmi[1] and S. Parthiban[2]*

[1]Research Scholar, Department of Chemistry, Annamalai University, Annamalainagar 608 002, Tamilnadu, India
[2]Assistant Professor, Department of Chemistry, Annamalai University, Annamalainagar 608 002, Tamilnadu, India

Abstract : Ammonium dihydrogen phosphate (ADP) is an available inorganic non-linear optical material needed for laser radiation. The beneficial optical crystals of pure, Fe (II) and Fe (III) (1 mol %) doped ADP crystals were obtained by slow evaporation solution growth technique (SEST). Well acquired crystals were characterized by different experimental techniques. Powder X-ray diffraction (XRD) and Fourier transform-infra-red (FT-IR) spectral studies substantiate the slight distortion of the crystal structure due to doping. The thermo-gravimetric and differential thermal analysis (TG-DTA) studies expose the pureness of the grown crystals. Scanning electron microscopic (SEM) analysis brings out the changes in the surface morphology because of doping. Optical studies were carried out by diffuse reflectance spectra (DRS). The second harmonic generation (SHG) efficiency, an essential requirement for the single crystals to identify the non-linear optical property was carried out by Kurtz powder technique.
Keywords ADP, non-linear optical, SEST, SHG.

1. Introduction

Ammonium dihydrogen phosphate (ADP), also known as monoammonium phosphate (MAP) is a distinguished non-linear optical (NLO) active crystal. It crystallizes in tetragonal geometry and it belongs to I-42d space group. Non-linear optical materials play an indispensable role in the fields of telecommunication, optical switching, optical processing, electro-optics, photonics and so on [1, 2]. ADP crystals are piezo-electric, which is a property required in some active sonar transducers [3]. Growth and characterization of crystals has been gained a noteworthy interest for the past two decades [4-9]. More and more brand-new concepts are come in to existence everyday that requires a novel ideas towards the exploration of new materials. Crystals are grown using both organic and inorganic materials. Inorganic materials are drawing special attention in the field of crystal growth [10]. Doping also has a positive results in the growth of crystals. Previously ADP was doped with both organic and inorganic dopants [11-14]. Doping Fe ions in the $LiNbO_3$ crystal has change the properties remarkably [15]. Transition metal ions doping on ADP always given an amusive and supportive results [16- 18]. The main objective of the present work is to harvest optically active and limpid, good quality ADP crystals by doping Fe with different oxidation states Fe(II) and Fe(III) and to depict the influence of Fe ions in ADP. A comparative study was done for all grown crystals *viz,* ADP, ADP/Fe(II), ADP/Fe(III) by using FT-IR, Powder-XRD, TG-DTA, SEM, EDX, and UV, characterization techniques.

2. Experimental techniques

2.1. Crystal Growth

Pure ADP and Fe ions with different oxidation states Fe(II) and Fe(III) doped ADP crystals were grown by slow evaporation solution growth technique. Pure ADP solution was prepared by adding saturated amount of ADP in 100 ml of doubly-distilled water. The prepared solution was allowed to stirred under magnetic stirrer for 3-4 hours at room temperature. After continuous stirring, the resulted solution was filtered in to a beaker and kept undisturbed for the growth of crystals. For doped product, 1 mol % of Fe(II) in the form of ferrous sulphate and Fe(III) in the form of ferric chloride were added separately to the saturated ADP solution, stirred and kept for crystallization process. Crystals were grown within 10-15 days. The addition of marginal quantity of dopant enhanced the growth of high quality transparent crystals. The grown crystals are further subjected to various characterization techniques. Photographs of the grown crystals are shown.

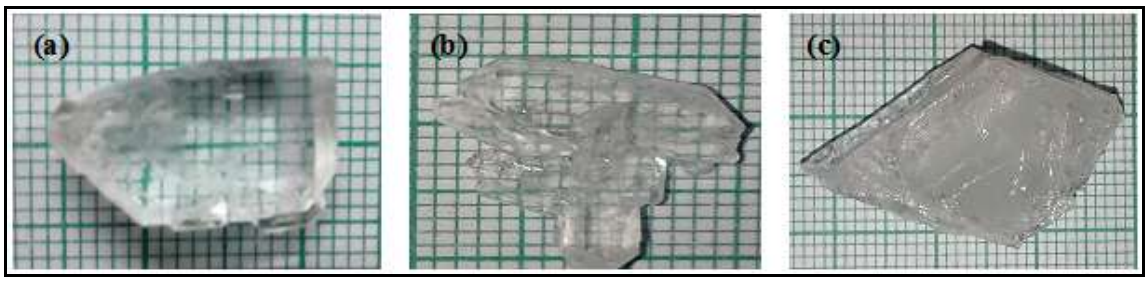

Fig. 1. Photographs of ADP crystals: (a) pure ADP, (b) 1 mol % of Fe(II) doped ADP, (c) 1 mol % of Fe(III) doped ADP.

2.2. Characterization

The FT-IR was observed for pure and Fe(II)/Fe(III) doped ADP by employing an AVATAR 330 FT-IR instrument by KBr pellet technique in the ambit of 500-4000 cm^{-1}. Powder X-ray diffraction is efficacious to substantiate the identity of a solid material and to ascertain the crystallinity and phase purity. The powder XRD was taken with the help of Philips Xpert Pro Triple-axis X-ray diffractometer using graphite monochromated Cu Kα radiation. The single-crystal XRD data was obtained by AXS (Kappa Apex II) X-ray diffractometer. Single-crystal XRD data were gathered on a diffraction system, which utilizes graphite monochromated MoKα (K= 0.71073 Å). UV-Visible spectra were recorded using a Hitachi UV-VIS spectrophotometer in the spectral range of 250-800 nm. Thermo-gravimetric and differential thermal analysis curve were recorded using NETZSCH STA 449F3 thermal analyzer at a heating rate of 10°C min^{-1} at room temperature to 600°C applying alumina crucibles with 15 mg of samples.

The surface morphology was found with the help of Carl Zeiss EVO 18 SEM. In the SEM, the icon was formed and laid out by a very fine electron beam, which is focused on the on the surface of the specimen. At any given moment, the specimen is bombarded with electrons over a very diminutive area. EDS is a chemical microanalysis technique performed in coincidence with SEM. Energy Dispersive X-ray spectrometer was taken by using Quantax 200 with X-flash- Bruker. This method is useful discover the elements present in the compound. This method can detect elements from Na upward in the periodic table. The second harmonic generation (SHG) test on the grown crystals was executed by the Kurtz powder SHG method [19]. A Nd:YAG laser with modulated radiation of 1064 nm was used as the optical source and directed on the powdered sample through a filter. The harvested crystals were ground to a unvarying particle size of 125-150 nm. After that, they were jammed in a microcapillary of uniform bore and subjected to laser radiation. The output signal from the sample was monochromated to compile the intensity of 532 nm component and to obviate the fundamental.

3. Results and discussion

3.1. FT-IR

The characteristic vibrational frequency of pure ADP and 1 mol % Fe(II) and Fe(III) doped ADP crystals are compared (Fig. 2). It indicates that the percentage of transmittance is lower in the case of Fe(III)

doping. The –NH group hydrogen stretching frequency at 3500 – 3000 cm^{-1} is a bit widened in the presence of Fe(III) doping and it pointed out the interaction between the Fe(III) dopant and –NH group of ADP. The intensity of the peak for pure ADP, Fe(II) and Fe(III) doped ADP appeared very sharp in the region of 1400 cm^{-1} and it illustrates the interstitial occupancy of both dopants in the crystal lattice without causing much strain to pure ADP and also due to absence of H- bonding.

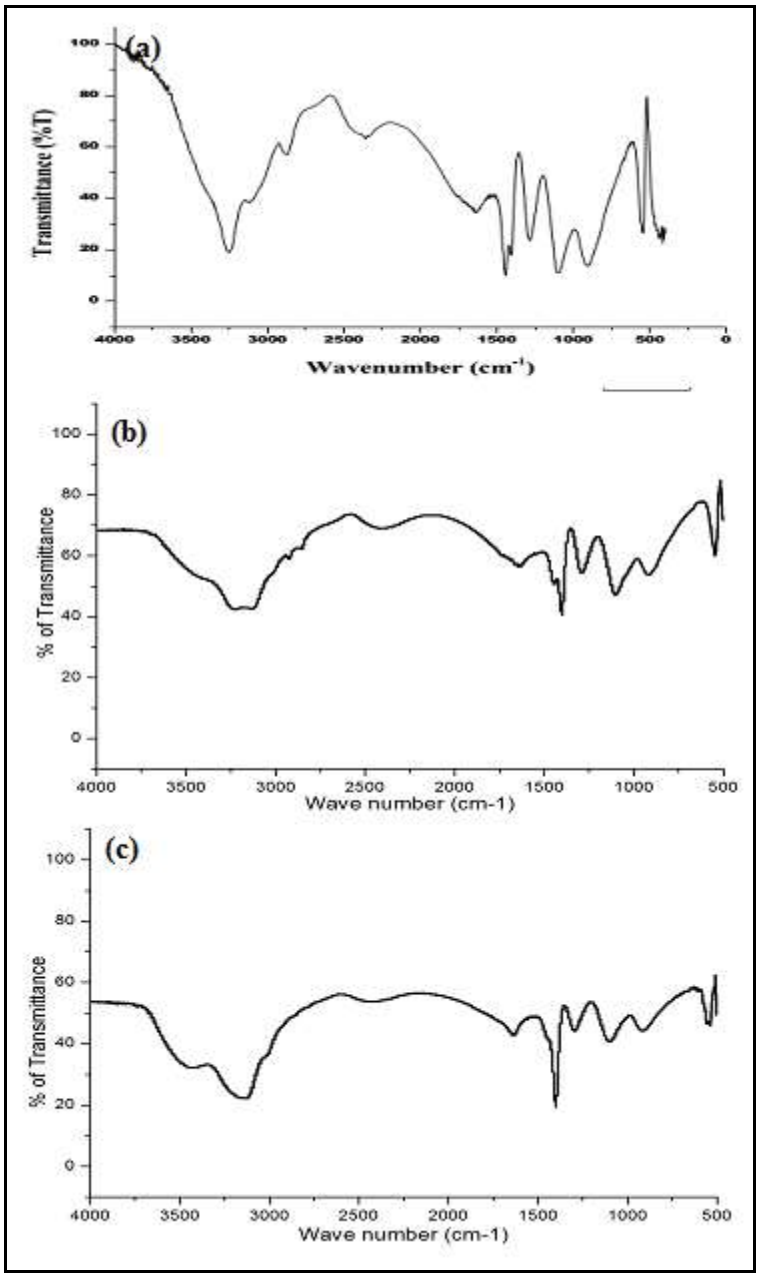

Fig. 2. FT-IR spectra of ADP crystals: (a) pure, (b) Fe(II)/ADP and (c) Fe(III)/ADP

3.2. UV Visible spectroscopic analysis

The UV–Vis spectra of Fe(II) and Fe(III) doped ADP crystals were observed and presented (Fig. 3). The figure shows that the absorption positions of Fe(II) and Fe(III) doped ADP crystals have no remarkable change from that of pure ADP crystal and the lower cut off wavelength for pure ADP is across 215 nm.

The diffuse reflectance spectra of Fe(II), and Fe(III) doped samples are shown (Fig. 4). Dopants are showing high reflectance in the whole visible region. The energy gap value Eg calculated by analyzing the optical data recorded with optical transmission coefficient and the photon energy. The band gap values of the

crystals are found (Table 1). The band gap value decreases in the presence of dopants which confirms incorporation of dopant in to the crystal lattice. Metallic dopants always decrease the transmittance values [20].

Table 1. Band gap for pure and doped crystals

Sample	Cut off Wavelength (nm)	Band gap (eV)
Pure ADP	215	6.16
Fe(II)/ADP	230	5.80
Fe(III)/ADP	230	5.98

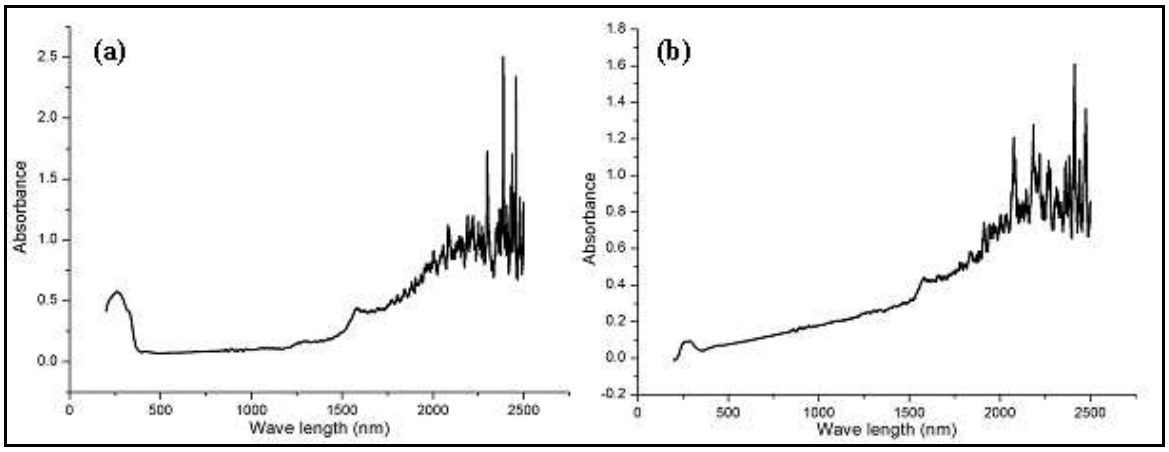

Fig. 3. UV-Visible spectra: (a) Fe(II)/ADP, (b) Fe(III)/ADP

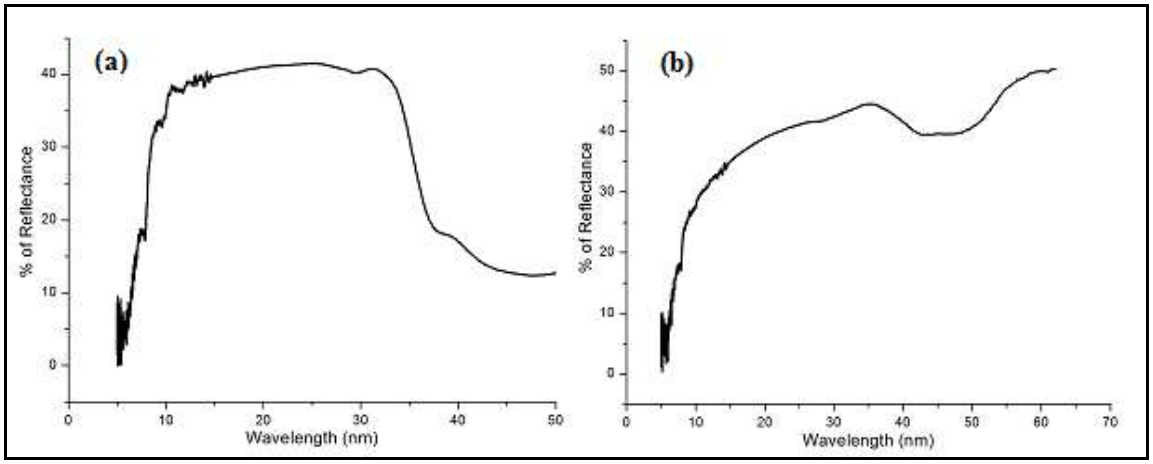

Fig 4. DRS: (a) Fe(II)/ADP, (b) Fe(III)/ADP

3.3. Powder and Single crystal X-ray diffraction

Powder X-ray diffraction studies of pure ADP, Fe(II) and Fe(III) doped ADP are compared (Fig. 5). XRD patterns of Fe(II) and Fe(III) doped samples are same as that of the patterns of pure ADP. Therefore it indicates that there is no change in the basic structure of ADP. Overall observation includes that there is a intensity reduction and little shift in the position of the peak for Fe(II) and Fe(III) doped ADP samples. This small shift could be due to the occupancy of dopants in the pure ADP crystal. It sustain that the Fe doping doesnot curb the growth of the crystals. The ionic radii of dopant iron in Fe(II) and Fe(III) is 75 and 65 pm respectively which is comparably less than that of the ionic radius of ammonium ion (143 pm) and hence it is well founded to accept that Fe occupies predominantly in the interstitial positions. It is evident from the lattice parameter values obtained using single-crystal XRD (Table 2), there is no new compound formation as the crystal system and lattice parameter values are not much altered [21]. A small change could be due to lattice strain.

Table 2. Lattice parameter values of pure ADP and Fe(II), Fe(III) doped ADP crystals

Crystal	a/Å	b/Å	c/Å	V/ Å^3	System
Pure ADP	7.502	7.512	7.566	428.6	Tetragonal
Fe(II)/ADP	7.516	7.516	7.516	424.5	Tetragonal
Fe(III)/ADP	7.690	7.690	7.690	454.8	Tetragonal

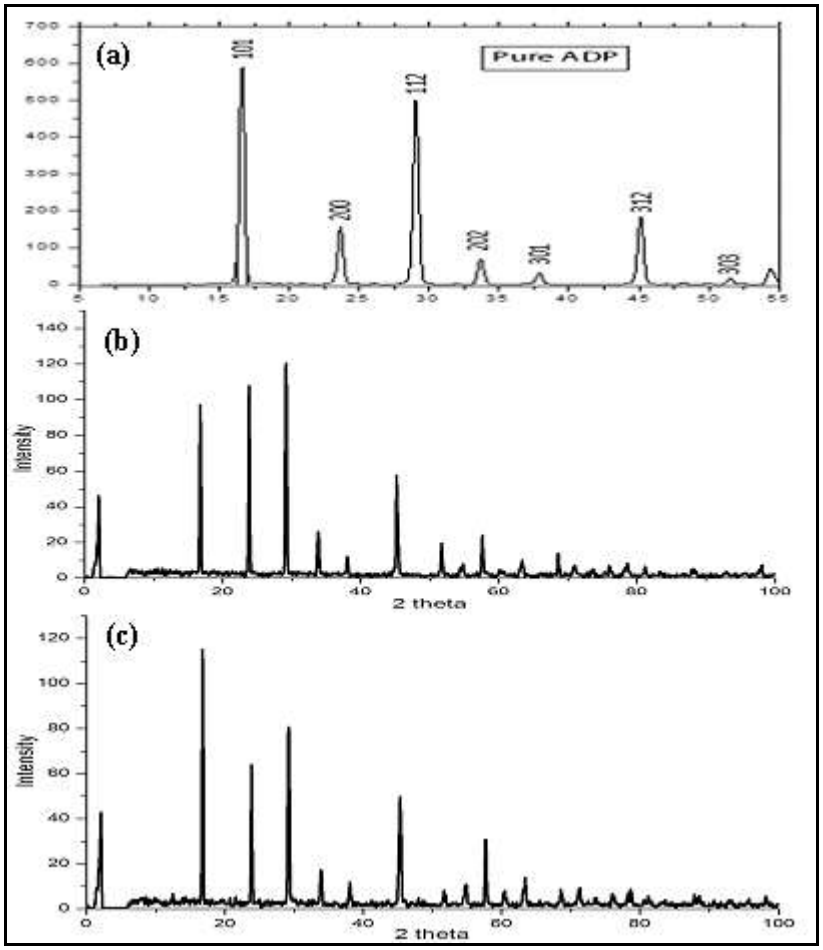

Fig. 5. Powder XRD patterns: (a) pure ADP, (b) Fe(II)/ADP and (c) Fe(III)/ADP

3.4. Thermal studies

Thermogravimetric and differential thermal analyses afford data with regard to phase transition, water of crystallization and different stages of decomposition of the substance. The thermogravimetric analysis of pure ADP, Fe(II) and Fe(III) doped ADP crystals was carried out between 50 – 500 °C in the nitrogen atmosphere at a heating rate of 10 °C min^{-1}. Figure 6 renders the TG-DTA curves of pure and Fe(II), Fe(III) doped ADP crystals. The TG curve of pure ADP reveals that the crystal is stable up to 190 °C, which is the melting point of ADP. In DTA analysis, absence of wide endothermic peak below 150 °C could be due to the absence of hygroscopic water in the crystal lattice. In the DTA curve of pure ADP and Fe(II), Fe(III) doped ADP, the endothermic peak starts at around 205, 220, 210 °C respectively (Table 3). At this particular temperature the crystals are started to decompose in to ammonia and phosphoric acid according to the following reaction,[22]

$$(NH_4)H_2PO_4\ \mathbf{(s)} \rightleftharpoons NH_3\ (g) + H_3PO_4 \qquad (2)$$

Table 3. Thermal analysis data of the crystals

Crystal	Endothermic peak/ °C	Decomposition temperature/°C
Pure ADP	205	190
Fe(II)/ADP	220	210
Fe(III)/ADP	210	195

Phosphoric acid boils at 213°C. It shows that after the decomposition of ADP in to ammonia and phosphoric acid, phosphoric acid again undergoes boiling and then it further starts to decompose up to 500°C. The decomposition temperature of the crystal is ever known by the formation of endothermic peaks [23]. It appears that, dopant slightly increased the decomposition of ADP crystals predominantly in the Fe(II) doped ADP.

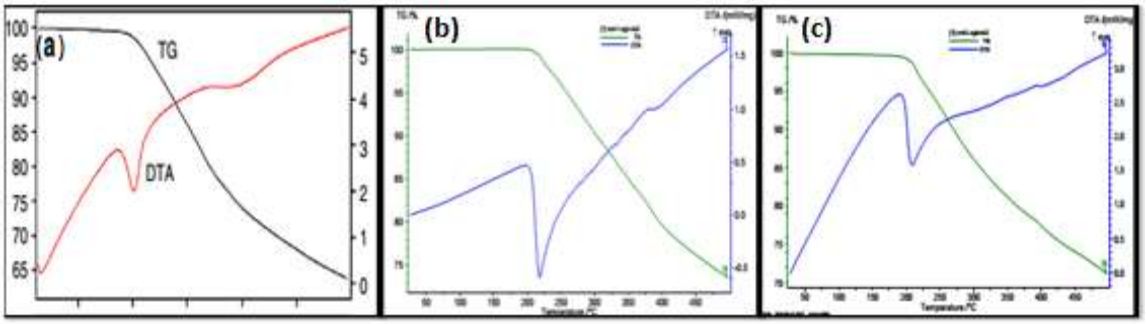

Fig. 6. TG-DTA curves of ADP crystals: (a) pure, (b) Fe(II) doped and (c) Fe(III) doped

3.5. SEM and EDS

Scanning electron microscopy gives information about the surface nature and its suitability for device fabrication. SEM is also used to investigate the presence of imperfections. The SEM photographs of pure ADP and Fe(II), Fe(III) doped ADP are shown (Fig. 7). Samples are having distinct morphology with different structural defect centres [24]. The SEM image of pure ADP looks like a layered structure. The SEM image of Fe(II) doped ADP reveals the dopant is aggregated at one common point of the lattice as bunched hillocks. In the case of Fe(III) doped ADP, agglomeration of dopants occurred. Energy dispersive X-ray spectroscopy is useful to confirm the presence of dopants. The amount of incorporation of Fe(II) and Fe(III) in to ADP crystal lattice is revealed by EDS (Fig. 8). Table 4 shows the total percentage of elements present in the crystal lattice. From the table, the amount of dopant present in the crystal is high for higher oxidation state of Fe. The amount of dopant occupying the lattice is increased as indicated by EDS.

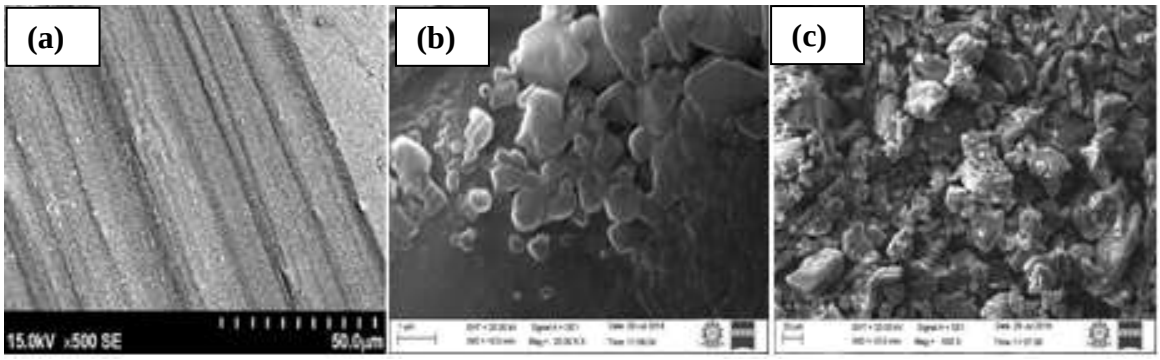

Fig. 7. SEM images: (a) pure ADP, (b) Fe(II)/ADP and (c) Fe(III)/ADP

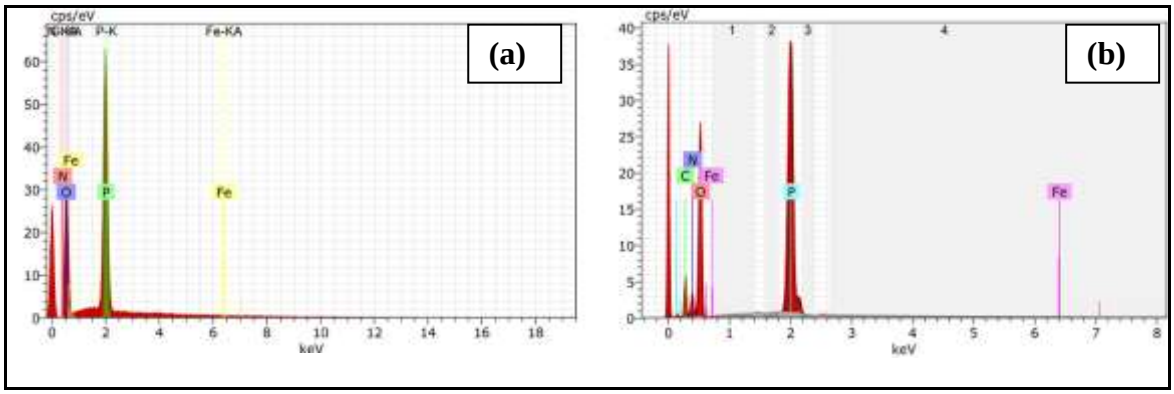

Fig. 8. EDS images: (a) Fe(II)/ADP and (b) Fe(III)/ADP

Table 4. EDS data of Fe(II)/ADP and Fe(III)/ADP

Element	Fe(II)/ADP		Fe(III)/ADP	
	Weight %	**Atomic %**	**Weight %**	**Atomic %**
Oxygen	21.94	64.71	22.82	67.40
Nitrogen	6.72	20.33	7.75	22.25
Phosphorous	2.87	11.99	2.32	10.33
Fe	0.08	0.01	0.10	0.03

3.6. SHG analysis

SHG efficiency is an important property to describe a crystal as a potential NLO crystal, analyzed by using Kurtz powder technique. A Nd:YAG laser with a modulated radiation of wavelength 1064 nm was taken as the optical source and passed on the powdered samples through a filter. The SHG efficiency of the samples were confirmed by the doubling of frequency by green radiation of wavelength 532 nm.

4. Conclusions

The characteristic results of Fe(II) and Fe(III) doped ADP crystals are presented. Crystals with good crystalline perfection are prepared by slow evaporation solution growth technique method. Slight changes in the FT-IR spectra of doped samples are observed when compared to pure ADP crystal. The sight occupancy of Fe(III) doped ADP is more compared to Fe(II) doped ADP as let out by EDS studies. The Fe(II) and Fe(III) doped ADP crystals shows high transparency in the entire UV-Visible region. Doping of Fe(II) and Fe(III) divulge the presence of various SEM morphologies. TG-DTA studies reveals that Fe(II) doped ADP crystal has greater decomposition starting temperature and both the crystals were grown by the absence of any adsorbed water molecules. Powder XRD patterns apparently brings out that the dopants has not altered the basic structure of ADP crystals. Possibly, the dopants occupy the interstitial position and influencing the properties. Besides, in the single crystal XRD studies there is only a slight change in the lattice parameter values as compared with the values of pure ADP. Since the Fe(II) and Fe(III) doped ADP crystals show lower band gap than pure ADP crystal, it can have high optical transmission. Second harmonic generation efficiency of Fe(II) and Fe(III) doped ADP crystals brings out that they have good potential for NLO applications since they show green light with a radiation of 532 nm using Nd:YAG laser.

References

1. Felicita Vimala J., Thomas Joseph Prakash J., Growth and characterization of Pure and Glycine doped Zinc thiourea chloride, Elixircrystal growth, 2013, 56; 13355-13358.
2. Hussaini S. S., Dhumane N. R., Dongre V. G., Karmuse P., Ghughare P. and Shirsat M. D., Effect of glycine on the optical properties of Zinc Thiourea Chloride (ZTC) single crystal, Opto electronics and Advanced Materials. Rapid Communications, 2008, 2; 108-112.

3. Yariv A., Yeh P., Optical waves in crystals. NewYork: Wiley, 1984; 69–120.
4. Prem Anand D., Gulam Mohamed M., Rajasekar S. A., Selvakumar S., Joseph Arul Pragasam A, Sathyaraj P, Growth and characterization of pure, Benzophenone and Iodine doped Benzoyl Glycine single crystals, Mater. Chem. Phys., 2006, 97; 501-105.
5. Shirsat M. D., Hussaini S. S., Dhumane N. R., Dongre V. G., Influence of lithium ions on the NLO properties of KDP single Crystals, Cryst. Res. Technol. 43 (2008), 756-761.
6. Hussaini S. S., Dhumane N. R., Dongre V. G., Karmuse P., Ghugare P., Shirsat M. D., Growth and characterization of glycine doped KDP single crystal for optoelectronics applications, J. Opt. Elect. Avv. Mater., (rapid comm.), 2007,12; 707-711.
7. Hussaini S. S., Dhumane N. R., Dongre V. G., Karmuse P., Ghugare P., Shirsat M. D., Effect of glycine on the optical properties of Zinc Thiourea Chloride (ZTC) single crystal, J. Opt. Elect. Avv. Mater. (rapid comm.), 2008, 1; 108-112.
8. Meera K., Muralitharan R., Dhanasekaran R., Manyum Prapun, Ramasamy P., Growth of nonlinear optical material: L-arginine hydrochloride and its characterization, J. Cryst. Growth., 2004, 263; 510-516.
9. Mohan Kumar R., Rajan Babu D., Jayaraman D., Jayavel R., Kitmura K., Studies on the growth aspects of semi-organic L-alanine acetate: a promising NLO crystal, J. Cryst. Growth., 2005, 275; 1-2.
10. Palanisamy S., Balasundaram O. N., Growth and Characterization of Nonlinear Optical Material: Glycine Sodium Chloride, Rasayan J. Chem., 2009, 2; 49-52.
11. Meenakshi Sundaram S. P., Parthiban S., Madhurambal G., Dhanasekaran R., and Mojumdar S. C., Effect of complexing agent (1, 10-phenanthroline) on ADP and KDP crystals, J. Therm. Anal. Cal., 2008, 94; 15-20.
12. Bhagavannarayana G., Parthiban S. and Subbiah Meenakshisundaram, Enhancement of crystalline perfection by organic dopants in ZTS, ADP and KHP crystals as investigated by high-resolution XRD and SEM. J. Appl. Cryst., 2006, 39; 784-790.
13. Bhagavannarayana G., Parthiban S. and Subbiah Meenakshisundaram, An interesting correlation between Crystalline Perfection and Second Harmonic Generation Efficiency on KCl and Oxalic acid doped ADP crystals, Crystal Growth & Design, 2008, 8; 446-451.
14. Girija P. and Parthiban S., J. Chem. & Chem. Sci., Comparative study of pure and Manganese doped Ammonium Dihydrogen Phosphate (ADP) crystals, 2015, 5; 253-258.
15. Pracka I., Bajor A. L., Kaczmarek S. M., Wirkowicz M., Kaczmarek B., Kisielewski J., Ukasiewicz T., Growth and characterization of $LiNbO_3$ single crystals doped with Cu and Fe ions, Cryst. Res Technol., 1999, 34; 627-634.
16. Bhagavannarayana G., Parthiban S., Meenakshisundaram S., An interesting correlation between Crystalline Perfection and Second Harmonic Generation Efficiency on KCl and Oxalic acid doped ADP crystals, Crystal Growth & Design, 2008, 8; 446-451.
17. Vanchinathan K., Muthu K., Bhagavannarayana G., Meenakshisundaram SP., Growth of cerium(III) doped ADP crystals and characterization studies, J. Cryst. Growth., 2012, 354; 57-61.
18. Rajesh P., Ramasamy P., Bhagavannarayana G., Kumar B., Growth of 1 0 0 directed ADP crystal with slotted ampoule. Current Applied Physics Curr. Appl, Phys., 2010. 10; 1221-1226.
19. Kurtz S. K., Perry T. T., A Powder technique for the evaluation of Nonlinear Optical Materials, J Appl. Phys., 1968, *39*; 3798–3813.
20. Amutha M., Ramasamy G., Meenakshisundaram S. P, Mojumdar S. C., Effect of s-, p-, d-, and f- block elements on the structure and properties of ammonium dihydrogen phosphate crystals, J. Therm. Anal. Calorim., 2011, 104; 949-954.
21. Voronov A. P., Vyday Y. T., Salo V. I., Puzikov V. M., Bondarenko S. I., Influence of Thallium doping on scintillation characteristics of mixed KDP/ADP crystals, Radiat. Meas., 2007, 42; 553-556.
22. Punitha P., et al. Influence of Cd(II) doping on the thermal and optical properties of ammonium dihydrogen phosphate crystals, J. Therm. Anal. Cal., 2014,10.1007/s10973-014-4131-6.
23. Rajesh P., Ramasamy P., Effect of oxalic acid on the optical, thermal, dielectric and mechanical behavior of ADP crystals, Phys. B., 2009, 404; 1611-1616
24. Kasthuri L., Bhagavannarayana G., Parthiban S., Ramasamy G., Muthu K., Meenakshisundaram SP, Rare earth cerium doping effects in non linear optical materials: potassium hydrogen phthalate (KHP) and tris thiourea zinc (II) sulfate (ZTS), Cryst. Eng. Comm., 2010, 12; 493-499.

*****